

Influence of light intensity on the kinetics of light-driven hydrogen evolution using Rh-doped SrTiO₃: a study by photoelectrochemical impedance spectroscopy

M. Antuch¹, A. Kudo², P. Millet^{1*}

¹ ICMMO-ERIEE (UMR CNRS 8182), Université Paris Sud, 91405 Orsay, France

² Department of Applied Chemistry, Tokyo University of Science, 1-3 Kagurazaka, Shinjuku-ku, Tokyo 162-8601, Japan

Received November 28, 2016 Revised March 6, 2017

Interest in the visible-light-driven hydrogen evolution reaction (HER) is nowadays determined by the urgent need for clean energy carriers. The mechanism of HER is known to be multistep, and is generally a bottleneck displaying kinetic hindrance. In this work, we report on the kinetics of the HER using a rhodium-doped strontium titanate (Rh:SrTiO₃) as photoactive material. In particular, we have been interested in determining the influence of light intensity (68-529 mW/cm² at 450 nm) on the kinetic parameters of the system. We observed that increasing light intensity yielded a slight increase in electron-hole recombination rate, because of the increasing amount of photo-generated electrons at the surface of the photo-electrode. We also found that the rate constant of the charge transfer process was independent of light intensity. The increase of electron-hole recombination determined the efficiency loss of the system when light was intensified. This work provides insights into the kinetics of charge transfer at photo-excited Rh:SrTiO₃/electrolyte interfaces, and also provides guidance for photoelectrochemical kinetic studies performed with photoelectrochemical impedance spectroscopy (PEIS).

Key words: hydrogen evolution, photoelectrochemical impedance spectroscopy, kinetics, doped strontium titanate.

INTRODUCTION

Increasing energetic demands of modern society, along with the exhaustion of carbon based fuels, has turned the attention of the scientific community to develop alternative, sustainable and low cost energetic sources [1]. In this context, the use of semiconductors, photoactive upon visible-light excitation, is a promising route [2-6]. Among all possible energetic applications of semiconducting electrodes, the study of the hydrogen evolution reaction (HER) is still a hot-spot [7-12] because of its possibilities of changing the planet energetic dependence for a fully clean source.

These facts prompted us to study the kinetics of the novel advanced semiconducting material (Rh doped SrTiO₃) that absorbs visible light, and has recently been shown to act as a potentially interesting hydrogen evolving photo-catalyst [13-16]. However, multistep charge transfer reactions, such as the HER, display poor kinetics, which determines the importance of unraveling the kinetic parameters behind the performance of this photoelectrocatalytic material.

Herein we present a kinetic study of the surface reactivity of Rh:SrTiO₃ ($E_g = 2.4$ eV, [13]) by photoelectrochemical impedance spectroscopy (PEIS), a technique originally developed by Ponomarev and Peter [17]. We were interested in particular at measuring the effect of light intensity on the kinetic parameters at constant applied potential. A theoretical background and the appropriate references to the models we employed in this work for data analysis are provided.

METHODS

SrTiO₃ powder doped with 1 mol % Rh at Ti sites was prepared by a solid-state reaction. The starting materials, SrCO₃ (Kanto Chemical; 99.9%), TiO₂ (Soekawa Chemical; 99.9%), and Rh₂O₃ (Wako Pure Chemical), were mixed in a Sr:Ti:Rh ratio of 1.07:(1-x):x. The mixture was calcined in air at 1173 K for 1 h and then at 1373 K for 10 h in an alumina crucible [13]. The chemical composition of the samples was determined using SEM-EDS Cambridge equipment and electron microprobe measurements (EPMA) (microprobe SX 100 CAMECA).

Photoelectrodes were prepared by drop-casting 10 μ L of an isopropanol suspension containing Rh:SrTiO₃ (30 mg in 0.5 mL) on top of an ITO surface. Next, 10 μ L of Nafion (50 μ L to a final volume of 1 mL in isopropanol) were put on top of

To whom all correspondence should be sent:
E-mail: pierre.millet@u-psud.fr

the surface through the same methodology, and let dry for three hours. In all cases, the solvent was let to evaporate at room temperature. Before measurements, photoelectrodes were put into Na₂SO₄ (0.1 M) solution and allowed to wet overnight. All electrochemical measurements were performed in aqueous Na₂SO₄ (0.1 M) in a three electrode cell configuration employing ITO-Rh:SrTiO₃-Nafion, saturated calomel electrode (SCE) and a carbon plaque, as working, reference and counter electrodes, respectively. MilliQ water was employed for all tests, and was obtained from a Merck Millipore device.

Photoelectrochemical impedance (PEIS) determinations were performed in a quartz photoelectrochemical cell from Pine Research Instrument Company. Measurements were performed in a Modulab Solartron Analytical potentiostat, model 2100A. The light source was controlled with a calibrated optical bench (Thorlabs Inc. DC2100), equipped with a LED giving light of 450 nm. PEIS spectra were recorded under potentiostatic control in the frequency range of 300 kHz to 50.2 mHz, the amplitude of the sinusoidal potential perturbation was 10 mV in all cases. Fitting of experimental PEIS spectra was performed in Matlab R2014b, with home-made code.

THEORETICAL BACKGROUND

The interface between a semiconducting electrode and a solution is special since for a p-type semiconductor there is an accumulation of electrons at the interface associated with an electron exchange between the electrolyte and the material, whose driving force originates in equating the Fermi levels of the solution and the semiconductor. Such electron accumulation causes a downward bending of the valence and conduction band edges, when the electrode is biased at a potential negative to the flat-band potential (Figure 1a). As a consequence, when an electric potential (V) is applied, a part of V drops inside the solid material and the other part drops in the solution side. This fact contrasts with metallic electrodes in which all the applied potential drops within the solution. In general, the part of the solution where the electric potential drops, called the Helmholtz layer, has an associated capacitance (C_H). In an analogous manner, the space located inside the semiconducting material in which the potential drops, has an associated capacitance as well, the so-called space charge capacitance (C_{sc}). Excepting heavily doped semiconductors, C_H is much higher than C_{sc} . This fact determines that most of the overall potential drops inside the material (i.e., in

the space charge region) and not in the solution side of the interphase, i.e. $\phi_{sc} \gg \phi_H$, where ϕ_{sc} stands for the potential drop within the space charge, and ϕ_H represents the potential drop in the Helmholtz layer. Naturally $V = \phi_{sc} + \phi_H$. When a semiconducting electrode is illuminated by light with an energy $h\nu$ higher than its band gap, charge separation occurs and an electron-hole pair is consequently generated (Figure 1 a) [2-4,18]. Because of band bending, the electrons move towards the surface with a flux represented here as I_0 . At the surface, electrons can be transferred to the solution to reduce species in the nearby (in this work we aim at the reduction of water according to $2H_2O + 2e^- = H_2 + 2OH^-$ with a phenomenological rate constant k_t). Additionally, the electrons can recombine at the surface with photogenerated holes with a rate constant k_r .

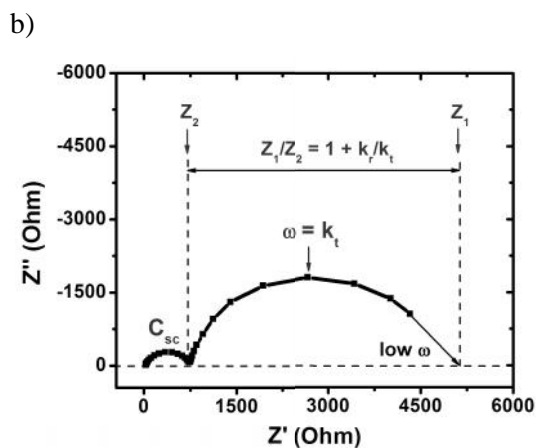
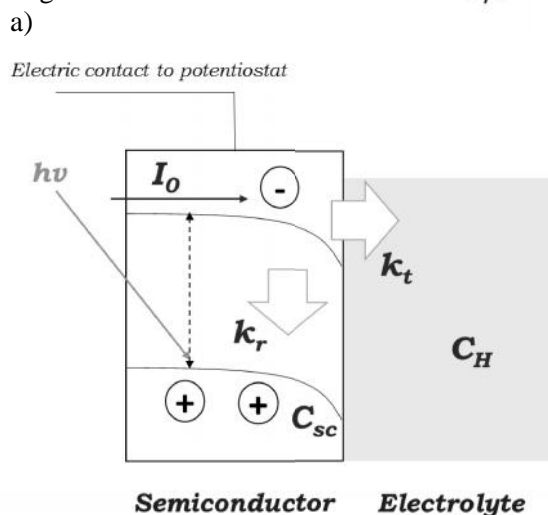


Fig. 1. a) Scheme of an illuminated p-type semiconductor under reverse bias. Main kinetic and photoelectrochemical parameters discussed in the text are presented; b) typical photoelectrochemical impedance spectrum (PEIS) of an illuminated semiconductor. The figure highlights how to determine the kinetics of light-driven reactions from PEIS (see text for explanations).

Understanding the kinetics of charge transfer and recombination in semiconducting electrodes is of paramount importance to continually improve their performance. In order to study the kinetics of charge transfer at Rh:SrTiO₃/electrolyte interfaces, we employed photoelectrochemical impedance spectroscopy (PEIS). PEIS consists in recording a usual EIS spectrum at a constant level of illumination. The space charge capacitance and the Helmholtz capacitance can be viewed as a part of two RC circuits in series, thus, the interfacial capacitance is $\frac{1}{C} = \frac{1}{C_{sc}} + \frac{1}{C_H}$. When $C_{sc} \ll C_H$, the overall capacitance is mostly due to the space charge and in such conditions experimental data may be fitted using Eq. (1). This permits to obtain a semi-quantitative evaluation of relevant transfer and recombination kinetic parameters (Figure 1) [19-20].

$$Z(\omega) = R + \frac{1}{i\omega C_{sc} + \left(\frac{q}{k_B T}\right) I_0 \left(\frac{k_r}{k_r + k_t}\right) \left(\frac{k_t + i\omega}{k_r + k_t}\right)} \quad (1)$$

In Eq. (1), ω is the angular frequency of the ac perturbation, $Z(\omega)$ represents the ω -dependent impedance of the interface in Ω , R corresponds to the ionic resistance of the solution in Ω , i is the imaginary unit, C_{sc} is the space-charge capacitance in F, q is the elemental charge, k_B stands for Boltzman's constant, T is the absolute temperature, I_0 is the photogenerated current of minority carriers (electrons in the case of a p-type semiconductor), k_r and k_t are the pseudo first order rate constants for recombination and charge transfer, respectively Eq. (1) describes two semicircles in the Nyquist plot.

For the case where the charge transfer rate constant does not depend on ϕ_H , the interface impedance $Z(\omega)$ tends to Z_1 at low frequencies (eq. 2).

$$\lim_{\omega \rightarrow 0} Z(\omega) = Z_1 = R + \frac{k_t + k_r}{\left(\frac{q}{k_B T}\right) I_0 k_r \left(1 + \frac{k_r}{k_t}\right)}, \quad (2)$$

where R is the resistance associated to the solution and the electric wiring.

The low frequency semicircle passes through a maximum from which the charge transfer rate constant k_t may be directly determined using Eq. 3:

$$\omega_1 = k_t \quad (3)$$

The high frequency limit of the low frequency semicircle is Z_2 given by Eq. (4):

$$Z_2 = R + \frac{k_r + k_t}{\left(\frac{q}{k_B T}\right) I_0 k_r} \quad (4)$$

Therefore, the ratio Z_1/Z_2 (Eq. 5) provides an estimation of k_r once k_t is known

$$\frac{Z_1 - R}{Z_2 - R} = 1 + \frac{k_r}{k_t} \quad (5)$$

Since the space charge capacitance and the Helmholtz capacitance are connected in series, the overall interface capacitance shall be determined by the lowest of both (i.e. C_{sc}). Thus, the high-frequency semicircle will provide an estimate of C_{sc} . The way PEIS may be used to extract all the above-mentioned kinetic parameters is summarized in Figure 1b.

Consequently, PEIS is a powerful technique to assess the kinetics at illuminated semiconducting electrodes, and getting information of the interfacial capacitances associated to the system.

RESULTS AND DISCUSSION

The first step we undertook was the characterization of the Rh:SrTiO₃ semiconducting material by means of Scanning Electron Microscopy (SEM) and Energy Dispersive Spectroscopy (EDS). Figure 2-a shows a SEM micrograph of the electrode surface. This is a microporous material in which the width of the space charge region is smaller than the particle size. Roughness effects have been disregarded in the analysis of PEIS spectra. In Figure 2 a, the Nafion film is not visible, indicating that it forms a very thin layer on top of the semiconducting powder. Additionally, the polycrystalline nature of the Rh:SrTiO₃ surface may be appreciated, as has been reported before [13]. Figure 2-b displays the EDS spectra of the ITO support compared to the semiconductor. The signals of the L-shells of In and Sn coming from ITO are well defined, and the Si K-shell is observed as well, which originates from the glass substrate on top of which ITO is deposited. In the case of the photoelectrode assembly, EDS revealed the presence of F at the surface, coming from Nafion. Additionally, the Sr and Rh L-shells, and Ti K-shell confirmed the identity of the semiconducting material.

Subsequently, the photoelectrochemical characterization was undertaken. The first interesting issue to note is that the PEIS spectra changed upon cycling. In particular, the spectra evolved from a broad semicircle (Figure 3 black) until the response stabilized providing two well defined semicircles (Figure 3-a, red). Such change indicates that the interface is changing with the electrochemical treatment. It could be caused either by the binding and accumulation of charged intermediates in surface states, or by chemical modification of the surface, as has been reported before [21]. Further photoelectrode surface characterization is required to deepen into the real

causes of the observed evolution of PEIS. These two facts would redistribute ϕ_{SC} and ϕ_H , thus changing C_{SC} and C_H , and hence modifying the appearance of PEIS diagrams. When a stable and reproducible PEIS spectrum was obtained, we proceeded to perform subsequent measurements at different light intensities, in order to unravel its effect upon the displayed kinetics.

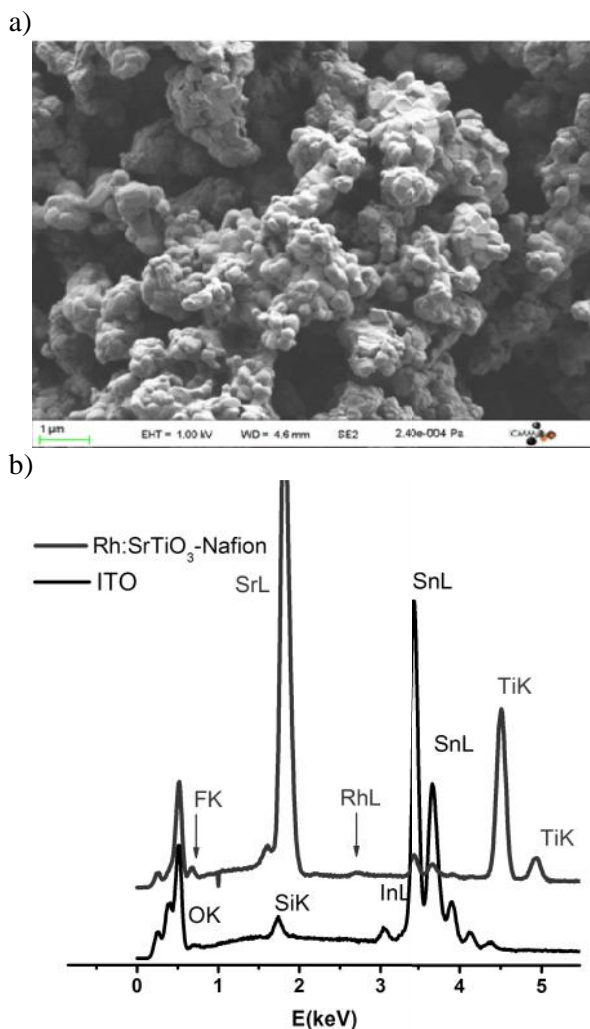


Fig. 2. a) SEM image of the electrode surface corresponding to Rh:SrTiO₃; b) EDS spectrum of the surface.

Figure 3-b shows the effect of light intensity upon the PEIS response of the photoelectrode. It may be perceived in Figure 3-b that the effect of light intensity on PEIS diagrams is small, but measurable, reproducible and reversible. No heat effect under illumination was identified. It follows a tendency in which an increase in light intensity provokes a shrinking of the high frequency semicircle and an expansion of the low frequency semicircle.

Before analyzing the PEIS results in the framework of the formalism exposed above in the theoretical section, it should be verified that

$C_{SC} \ll C_H$. The space charge capacitance was estimated initially by a fit of the high frequency semicircle (in the 300 kHz to 30 Hz frequency domain) to a RC circuit, yielding a value of $\sim 2.7 \cdot 10^{-7}$ F. Such value is small enough to ensure neglecting $1/C_H$ in front of $1/C_{SC}$.

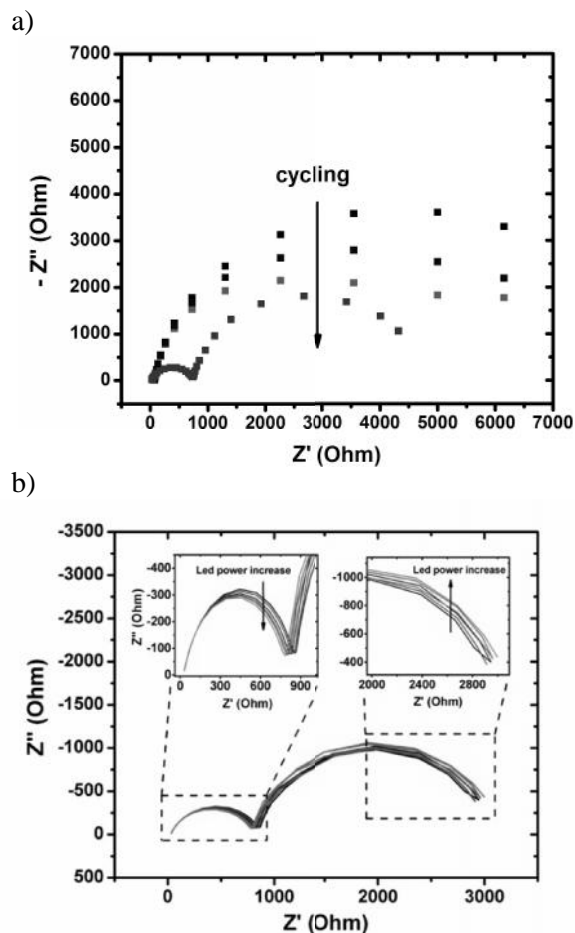


Fig. 3. a) Evolution of PEIS spectra of Rh:SrTiO₃ upon potential cycling at constant illumination. The red curve was found to be the stable response; b) Evolution of PEIS spectra at different light intensities. The sense of light increase is depicted in the insets. PEIS spectra were taken in the range of 300 kHz to 50.2 mHz at a constant applied potential of -1.25 V vs SCE. Light intensities were 67.9, 185.92, 294.13, 393.52, 485.34, 529.03 mW/cm².

To get detailed information, PEIS spectra were fitted to Eq. (1) with I_0 , C_{SC} , k_r and k_t as adjustable parameters. Fitting results are shown in Figure 4, where dashed lines have been put as a guide to the eye. For example, it may be appreciated that I_0 increases with increasing light intensity. This is a logical result since the flux of photogenerated electrons should become higher when light is made more intense. In the same way, the recombination rate constant showed a slight tendency to increase with light intensity (observed as a slight expansion of the low frequency semicircle in Figure 3-b).

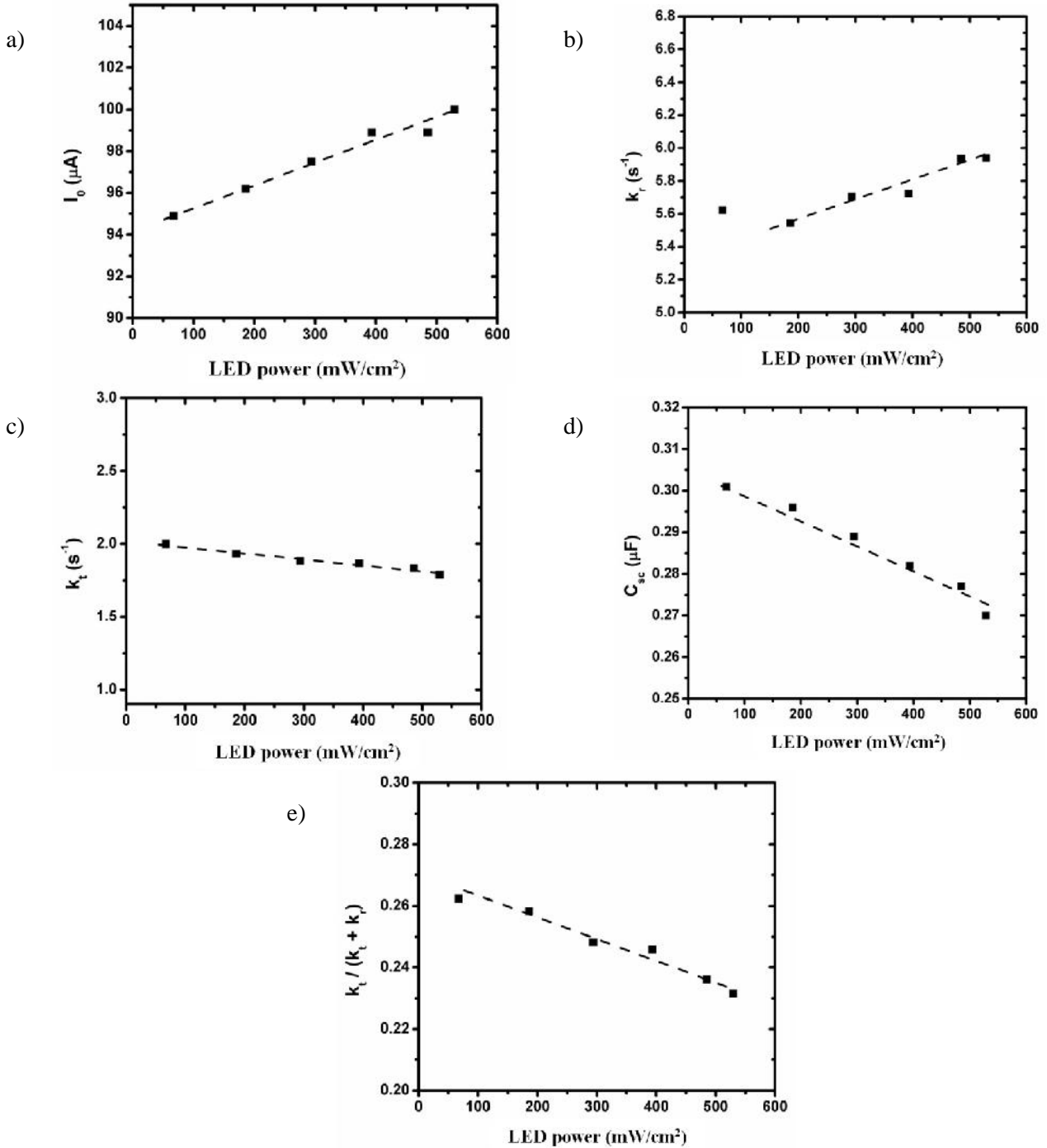


Fig. 4. Fitting results of PEIS spectra shown in Figure 3 b, to equation 1; Dependence with light intensity of: a) the flux of photogenerated minority carriers (I_0); b) the recombination rate constant (k_{rec}); c) the charge transfer rate constant; d) the space charge capacitance (C_{sc}) and e) the efficiency of the photoelectrode.

Considering that k_r is proportional to the electron surface concentration as shown in Eq. (6) [20],

$$k_r = k'_r n_{surf} = k_r^0 \exp\left(\frac{-q\phi_{sc}}{kT}\right), \quad (6)$$

where n_{surf} is the electron concentration at the surface of the electrode, k represents the Boltzmann's constant, T is the absolute temperature and q is the elemental charge.

It follows directly from Eq. (6) that further light power will increase the electron concentration at the surface of the semiconductor and hence the value of k_r , thus decreasing band bending (ϕ_{sc}). At a constant applied potential V , a decrease in ϕ_{sc} should be compensated by an increase in ϕ_H , which should be translated into an increase in k_t (Eq. 7)

$$k_t = k_t^0 \exp\left(\frac{q\phi_H}{kT}\right). \quad (7)$$

However, such an increase in k_t is not well defined and k_t appears to keep the same value in the whole range of light intensities tested here, suggesting that the electron concentration at the surface does not change much over the entire range of light intensities under consideration. Such behavior is characteristic of Fermi level pinning associated with the presence of surface states in the photoelectrode [19].

On the other hand, C_{sc} displays a decrease with LED power augmentation (Figure 4-d), a behavior observed before in semiconducting photoelectrodes [19]. This can be interpreted as follows: as light increases, more electrons go to the surface while the holes remaining inside the material create an opposing electric field that continually diminishes the band bending (ϕ_{sc}). According to Eq. (8), such fact would increase C_{sc} . Though, the rise in light intensity makes the electrons to be located at the surface and the holes migrate to the bulk (where no electric field exists), the net charge in the space charge region (Q_{sc}) diminishes as well, which appears to be the dominating factor to explain the observed trend in C_{sc} with increasing light intensity

$$C_{sc} = \frac{dQ_{sc}}{d\phi_{sc}}. \quad (8)$$

Finally, the fraction of photogenerated electrons that are indeed transferred to the electrolyte to evolve H₂ is given by Eq. (9), and provides a measure of the efficiency of the photoelectrode

$$\eta = \frac{k_t}{k_t + k_r}. \quad (9)$$

Figure 4-e shows a loss in photoelectrode efficiency as light becomes stronger, which is a cause of increased recombination upon intensification of incoming light.

CONCLUSIONS

In this work, we have studied the influence of light intensity on the kinetics of light-driven hydrogen evolution at Rh doped SrTiO₃ photoelectrode in sodium sulfate electrolyte. Photoelectrochemical impedance spectroscopy proved to be a powerful technique to determine the kinetic parameters of the system under different light intensities. As expected, the flux of photogenerated minority carriers (I_0) (i.e. the flux of electrons in p-type semiconductors under reversed bias) increased with light strengthening. Furthermore, we observed that the recombination rate constant (k_r) displayed a slight tendency to rise as light became more intense, which was interpreted to be related to the increasing concentration of electrons at the interface.

Conversely, the charge transfer rate constant k_r proved to be independent of light intensity, a characteristic known as light-induced Fermi level pinning. Stronger illumination caused a decrease in band bending (ϕ_{sc}) and in the charge within the space charge region (Q_{sc}), which determined a decrease in the space charge capacitance. Overall, the efficiency of the photoelectrode regarding the transformation of visible light into H₂ decreased as light became more intense, due to increased recombination rate.

REFERENCES

1. S. Chu, A. Majumdar, Opportunities and challenges for a sustainable energy future, *Nature*, 488, 294 (2012), doi:10.1038/nature11475.
2. D. Fabian, S. Hu, N. Singh, F. Houle, T. Hisatomi, K. Domen, F. Osterloh, S. Ardo, Particle Suspension Reactors and Materials for Solar-Driven Water Splitting, *Energy Environ. Sci.*, 8, 2825 (2015), doi:10.1039/C5EE01434D.
3. T. Hisatomi, J. Kubota, K. Domen, Recent advances in semiconductors for photocatalytic and photoelectrochemical water splitting., *Chem. Soc. Rev.*, 43, 7520 (2014), doi:10.1039/c3cs60378d.
4. J. Ran, J. Zhang, J. Yu, M. Jaroniec, S.Z. Qiao, Earth-abundant cocatalysts for semiconductor-based photocatalytic water splitting, *Chem. Soc. Rev.*, 43, 7787 (2014), doi:10.1039/c3cs60425j.
5. M. Schreier, J. Luo, P. Gao, T. Moehl, M.T. Mayer, M. Grätzel, Coordinative immobilization of a molecular catalyst on Cu₂O photocathodes for CO₂ reduction, *J. Am. Chem. Soc.*, 138, 1938 (2016), doi:10.1021/jacs.5b12157.
6. J. Swierk, T. Mallouk, Design and development of photoanodes for water-splitting dye-sensitized photoelectrochemical cells., *Chem. Soc. Rev.*, 42, 2357 (2013), doi:10.1039/c2cs35246j.
7. J. Saioa Cobo, P. Jacques, J. Fize, V. Fourmond, L. Guetaz, B. Jusselme, V. Ivanova, H. Dau, S. Palacin, M. Fontecave, V. Artero, A Janus, Cobalt-based catalytic material for electro-splitting of water, *Nat. Mater.*, 11, 802 (2012), doi:10.1038/nmat3385.
8. B. Rausch, M. Symes, G. Chisholm, L. Cronin, Decoupled catalytic hydrogen evolution from a molecular metal oxide redox mediator in water splitting, *Science*, 345, 1326 (2014).
9. E. Andreiadis, P. Jacques, P. Tran, A. Leyris, M. Chavarot-Kerlidou, B. Jusselme, M. Matheron, J. Pécaut, S. Palacin, M. Fontecave, V. Artero, Molecular engineering of a cobalt-based electrocatalytic nanomaterial for H₂ evolution under fully aqueous conditions, *Nat. Chem.*, 5, 48 (2013), doi:10.1038/nchem.1481.
10. R. Subbaraman, D. Tripkovic, D. Strmcnik, K. Chang, M. Uchimura, A. Paulikas, V. Stamenkovic, N. Markovic, Enhancing Hydrogen Evolution Activity in Water Splitting by Tailoring Li⁺-Ni(OH)₂-Pt Interfaces, *Science*, 334, 1256 (2011).

11. P.D. Tran, T. V. Tran, M. Orto, S. Torelli, Q.D. Truong, K. Nayuki, Y. Sasaki, S.Y. Chiam, R. Yi, I. Honma, J. Barber, V. Artero, Coordination polymer structure and revisited hydrogen evolution catalytic mechanism for amorphous molybdenum sulfide, *Nat. Mater.* (2016) just accepted, doi:10.1038/nmat4588.
12. J. Zheng, W. Sheng, Z. Zhuang, B. Xu, Y. Yan, Universal dependence of hydrogen oxidation and evolution reaction activity of platinum-group metals on pH and hydrogen binding energy, *Sci. Adv.*, 2, 1 (2016), doi:10.1126/sciadv.1501602.
13. K. Iwashina, A. Kudo, Rh-Doped SrTiO₃ Photocatalyst Electrode Showing Cathodic Photocurrent for Water Splitting under Visible-Light Irradiation, *J. Am. Chem. Soc.*, 133, 13272 (2011).
14. T.H. Qian Wang, Q. Jia, H. Tokudome, M. Zhong, C. Wang, Z. Pan, T. Takata, M. Nakabayashi, N. Shibata, Y. Li, I.D. Sharp, A. Kudo, T. Yamada, K. Domen, Scalable water splitting on particulate photocatalyst sheets with a solar-to-hydrogen energy conversion efficiency exceeding 1%, *Nat. Mater.* (2016) just accepted.
15. Q. Jia, A. Iwase, A. Kudo, BiVO₄-Ru/SrTiO₃:Rh composite Z-scheme photocatalyst for solar water splitting, *Chem. Sci.* 5 (2014) 1513–1519. doi:10.1039/C3SC52810C.
16. B. Zhang, X. Zhang, X. Xiao, Y. Shen, Photoelectrochemical Water Splitting System-A Study of Interfacial Charge Transfer with Scanning Electrochemical Microscopy, *ACS Appl. Mater. Interfaces.*, 8, 1606 (2016), doi:10.1021/acsami.5b07180.
17. E. Ponomarev, L. Peter, A Comparison of Intensity Modulated Photocurrent Spectroscopy and Photoelectrochemical Impedance Spectroscopy in a Study of Photoelectrochemical Hydrogen Evolution at p-InP, *J. Electroanal. Chem.*, 397, 45 (1995), doi:10.1016/0022-0728(95)04148-9.
18. T.W. Hamann, F. Gstrein, B.S. Brunchwitz, N.S. Lewis, Measurement of the driving force dependence of interfacial charge-transfer rate constants in response to pH changes at n-ZnO/H₂O interfaces, *Chem. Phys.*, 326, 15 (2006), doi:10.1016/j.chemphys.2006.02.027.
19. K. Upul Wijayantha, S. Saremi-Yarahmadi, L. Peter, Kinetics of oxygen evolution at -Fe₂O₃ photoanodes: a study by photoelectrochemical impedance spectroscopy, *Phys. Chem. Chem. Phys.*, 13, 5264 (2011), doi:10.1039/c0cp02408b.
20. W.H. Leng, Z. Zhang, J.Q. Zhang, C.N. Cao, Investigation of the Kinetics of a TiO₂ Photoelectrocatalytic Reaction Involving Charge Transfer and Recombination through Surface States by Electrochemical Impedance Spectroscopy, *J. Phys. Chem. B.*, 109, 15008 (2005), doi:10.1021/jp051821z.
21. H. Tan, Z. Zhao, W. Bin Zhu, E.N. Coker, B. Li, M. Zheng, W. Yu, H. Fan, Z. Sun, Oxygen Vacancy Enhanced Photocatalytic Activity of Pervoskite SrTiO₃, *ACS Appl. Mater. Interfaces.*, 6, 19184 (2014), doi:10.1021/am5051907.

	Rh-	SrTiO ₃ :
	1, 2, 1*	
¹ I	(8182),	, 91405
2	,	, 1-3
	28	6
	()	2017
	(HER)	
	HER	(Rh: SrTiO ₃)
	(68-529 mW/cm ²	450)
		e
	Rh:SrTiO ₃ /	
		(PEIS).